

ELECTRONIC SUPPLEMENTARY INFORMATION (ESI)

Platinum diimine-dithiolate complexes as a new class of photoconducting compounds for pristine photodetectors: case study on [Pt(bipy)(Naph-edt)] (bipy = 2,2'-bipyridine; Naph-edt²⁻ = 2-naphthylethylene-1,2-dithiolate)

M. Carla Aragoni,^a Massimiliano Arca,*^a Maddalena Binda,^b Claudia Caltagirone,^a Vito Lippolis,^a

Dario Natali,^{b,c} Enrico Podda,^a Marco Sampietro,^{b,c} and Anna Pintus*^a

^a Università degli Studi di Cagliari, Dipartimento di Scienze Chimiche e Geologiche, S.S. 554 bivio per Sestu, 09042 Monserrato (Cagliari), Italy. E-mail: apintus@unica.it, marca@unica.it

^b Center for Nano Science and Technology @Polimi, Istituto Italiano di Tecnologia, Via Pascoli 70/3, 20133 Milano, Italy

^c Politecnico di Milano, Dipartimento di Elettronica, Informazione e Bioingegneria, Via Ponzio 34/5, 20133 Milano, Italy

[‡] Current affiliation: Energy Everywhere Italy, Via Pascoli 70/3, 20133 Milano, Italy

EXPERIMENTAL SECTION

Materials and Methods. Solvents (reagent grade) and reagents were obtained from commercial sources, and when necessary purified according to standard techniques. When required, manipulations were performed using standard Schlenk techniques under dry nitrogen atmosphere. Cyclic voltammetry (CV) measurements were recorded at 25 °C in anhydrous CH₂Cl₂ at scan rate 0.1 V s⁻¹, using a Metrohm Autolab PGSTAT 10 potentiostat at 20 °C in a Metrohm voltammetric cell, with a combined working and counter Pt electrode and a standard Ag/AgCl (in KCl 3.5 M) reference electrode. All potentials are referred to the Fc⁺/Fc couple, used as an internal standard. Tetrabutylammonium hexafluorophosphate was used as a supporting electrolyte ($C = 1 \cdot 10^{-2}$ M). Absorption spectra were recorded at 25 °C in a quartz cell of 10.00 mm optical path with a Thermo Evolution 300 (190–1100 nm) spectrophotometer. Diffuse reflectance measurements were carried out on KBr diluted pellets on an Agilent Cary 5000 UV-Vis-NIR dual-beam spectrophotometer equipped with a diffuse reflectance accessory in the range 300–5000 nm. Spectra were corrected for the change in the detector (PMT and InGaAs) at 800 nm.

Synthesis. Compound **1** was synthesized according to a previously reported method:¹ an ethanol solution of KOH (15 mL; 0.070 g, 1.25 mmol) was added dropwise to 2-naphthyl-[1,3]dithiol-2-one² (15 mL of EtOH; 0.090 g, 0.35 mmol) under a dinitrogen inert atmosphere. An equimolar suspension of [Pt(2,2'-bipy)Cl₂]³ in THF (20 mL, 0.15 g; 0.35 mmol) was then added. The reaction mixture was kept under magnetic stirring for 7 days in the absence of light and under an inert atmosphere, in order to avoid photooxidation.⁴ The dark precipitate was filtered off and washed with ethanol and water. Yield: 0.13 g, 0.25 mmol (70%); m.p. > 240 °C; FT-IR (KBr pellet): $\tilde{\nu} = 475$ (s), 718 (m), 748 (s), 761 (m), 811 (m), 1098 (vs), 1260 (m), 1384 (m), 1430 (w), 1446 (m), 1468 (m), 1508 (w), 1523 (m), 1561 (w), 1571 (w), 1594 (m), 1603 (m), 1619 (m), 1624 (m), 1638 (w), 1648 (w), 1655 (w), 1686 (w), 1719 (w), 1735 (w), 2345 (m), 2364 (m), 2926 (w), 2962 (w), 3057 cm⁻¹ (vw); UV-Vis-NIR (DMSO): $\lambda (\varepsilon) = 261$ (27000), 301 (30000), 344 (11000), 381 (8400), 603 nm (6000 M⁻¹ cm⁻¹); ¹H-NMR (300 MHz, DMSO-d₆): $\delta =$

9.43 (d, 1H), 9.26 (d, 1H), 8.78 (d, 2H), 8.50 (t, 2H), 8.31 (s, 1H), 8.00 (t, 2H), 7.94 (m, 4H), 7.56 (m, 2H), 7.25 (s, 1H) ppm; elemental analysis calcd (%) for C₂₂H₁₆N₂S₂Pt: C 46.56, H 2.84, N 4.94, S 11.30; found: C 46.21, H 2.81, N 4.82, S 11.15.

Photoconductivity measurements. Photoconductivity measurements were performed by using prototype lateral devices prepared by casting a CH₂Cl₂ suspension ($C \approx 2 \text{ mg mL}^{-1}$) of complex **1** on a quartz substrate with previously lithographed gold electrodes with inter-electrode spacings $L = 6 \mu\text{m}$. The devices were kept in vacuum ($P < 10^{-3} \text{ mbar}$) and irradiated with a set of light emitting diodes (LEDs) emitting a power density of few hundreds of mW/cm² (calibration was obtained by means of a silicon photodetector). Photoconducting properties were investigated by applying an external bias voltage $V_{\text{BIAS}} = 60 \text{ V}$ and measuring the photocurrent by means of a transimpedance amplifier connected to an oscilloscope. In order to calculate the External Quantum Efficiency (EQE) we computed the ratio between the photocurrent divided by the unit charge q and the number of photons impinging on the device area per second.

Stability tests. UV-Vis spectra were recorded on solutions of complex **1** in DMSO, DMF, CH₂Cl₂, CHCl₃, and THF over 48 hours to verify their stability toward dioxygen photooxidation.⁴ All the solutions were stable over 2 hours. In the solid state the compounds were proved to be stable over several months.

In order to further investigate the stability of complex **1** in the solid state a sample was irradiated with a continuous class 2 red laser (650 nm; 30 mW/cm²) for 210 minutes. Diffuse reflectance spectra were collected before and after irradiation showing no remarkable differences in the spectral shape (Figure S8) under the same conditions described above.

Theoretical calculations. Theoretical calculations were performed at the density functional theory (DFT)⁵ level with the Gaussian 16 (Rev. B.01)⁶ suite of programs on a IBM x3755 server with four 12-core processors and 64 GB of RAM (OS: SUSE Linux Enterprise Server 11 SP3). The PBE0 functional⁷ was adopted, in combination with the full-electron split valence basis sets (BSs) including polarization

functions (def2-SVP)^{8,9} for light atomic species (C, H, N, S) and the CRENBL BS¹⁰ with effective core potentials¹¹ for platinum. Basis sets were obtained from Basis Set Exchange and Basis Set EMSL Library.¹²

In order to establish the more stable mutual orientation for the complex molecules in oligomeric systems, a series of preliminary calculations were performed on the assembly [Pt(bipy)(Naph-edt)]₂, which was optimized starting from three different configurations (all featuring the single complex units in their planar form), with one of the complex molecules generated by symmetry from the other: I) a head-to-tail orientation (symmetry transformation: $-x, -y, z+3.5$); II) a slipped head-to-tail configuration featuring the bipyridine ligands lying above each other (symmetry transformation: $-x+8, -y, z+3.5$); III) a head-to-head conformation (symmetry transformation: $-x, y, z+3.5$). After the geometry optimization, the complex units lost their planarity in all of the conformations considered (mostly due to the rotation of the naphthyl substituents), and a slight rearrangement in their reciprocal position occurred. The optimized geometry obtained starting from configuration I was observed to be the most stable (total electronic energy lower by 1.3 and 20.0 kcal mol⁻¹ with respect to the geometries obtained starting from II and III, respectively). The assembly **2**, built of four interacting complex units, was thus optimized starting from a configuration where the complex molecules were generated by symmetry in the same way as in I (symmetry transformations: $-x, -y, z+3.5; x, -y, z+7.0; -x, -y, z+10.0$). Tight SCF convergence criteria (*SCF = tight* keyword) and fine numerical integration grids (*integral = ultrafine* keyword) were used, and the nature of the minima of the optimized structure was verified by harmonic frequency calculations (*freq = raman* keyword). A natural population analysis was carried out at the optimized geometries using the natural bonding orbital [NBO; *pop = (full,nbo)* keyword] partitioning scheme.¹³ Electronic transition energies and oscillator strength values were calculated at TD-DFT level (200 states; *td = nstates = 200* keyword). The programs GaussView 6.0.16,¹⁴ Molden 6.2,¹⁵ and Chem3D Pro 4.53¹⁶ were used to investigate the optimized structures and the shapes of Kohn–Sham

molecular orbitals. The software GaussSum 2.1¹⁷ was used to calculate the molecular orbital contributions, along with the contributions of singly excited configurations to each electronic transition.

Table S1. Optimised geometry calculated for **1** at DFT level in the gas phase (total charge = 0, spin multiplicity = 1) in orthogonal Cartesian coordinate format (Z = atomic number).

Atom number	Z	x	y	z
1	6	0.020603	-0.030156	0.002079
2	6	0.018868	0.134341	1.368440
3	6	1.229975	0.110722	2.105360
4	6	2.463771	-0.085333	1.409811
5	6	2.430681	-0.257001	-0.000328
6	6	1.239673	-0.228815	-0.687831
7	6	1.272618	0.269788	3.514668
8	6	2.463064	0.245359	4.196958
9	6	3.702846	0.060389	3.518078
10	6	3.674399	-0.113988	2.142993
11	6	4.971005	0.061441	4.268083
12	6	6.149908	0.494772	3.754172
13	16	7.625559	0.489006	4.654898
14	78	7.054601	-0.351063	6.677056
15	16	4.928024	-0.526704	5.924332
16	7	6.689004	-1.093787	8.547631
17	6	7.768511	-1.149195	9.375234
18	6	7.643058	-1.632516	10.684475
19	6	6.410296	-2.061782	11.144558
20	6	5.312044	-2.001458	10.279209
21	6	5.493174	-1.514525	8.997931
22	6	9.018101	-0.679007	8.790009
23	6	10.245535	-0.653918	9.465429
24	6	11.378170	-0.191034	8.818439
25	6	11.264302	0.243107	7.492846
26	6	10.028065	0.196076	6.875400
27	7	8.924597	-0.251779	7.500939
28	1	8.516062	-1.669435	11.336225
29	1	6.300875	-2.440163	12.162811
30	1	4.319714	-2.329264	10.592460
31	1	4.665755	-1.449786	8.286626
32	1	10.305053	-0.999080	10.497713
33	1	12.339703	-0.167184	9.335024
34	1	12.126480	0.616311	6.938159
35	1	9.891475	0.523772	5.841634
36	1	6.216836	0.911083	2.745629
37	1	4.605163	-0.301547	1.601731
38	1	0.334623	0.421575	4.056180
39	1	2.477935	0.383834	5.280547
40	1	3.373324	-0.410764	-0.532860
41	1	1.231557	-0.360316	-1.772803
42	1	-0.919684	-0.009203	-0.554410
43	1	-0.920987	0.286268	1.906630

Table S2. Selected optimized bond lengths (\AA) and angles ($^\circ$) for **1** and the four complex a–d units within the assembly **2** (a–d) at the optimized geometry in the gas phase (labelling schemes as in Figures S3 and S5).

	1	2			
		a	b	c	d
Pt–N1	2.046	2.055	2.055	2.054	2.051
Pt–N2	2.046	2.050	2.053	2.054	2.055
Pt–S1	2.263	2.269	2.281	2.281	2.272
Pt–S2	2.263	2.271	2.276	2.275	2.268
N1–Pt–N2	79.21	79.19	79.24	79.27	79.06
S1–Pt–S2	88.20	88.38	88.42	88.42	88.30
N1–Pt–S1–C1	179.84	175.21	177.83	177.34	173.41
C1–C2–C3–C4	31.0	28.00	28.58	25.39	32.45

Table S3. Optimised geometry calculated for **2** at DFT level in the gas phase (total charge = 0, spin multiplicity = 1) in orthogonal Cartesian coordinate format (Z = atomic number).

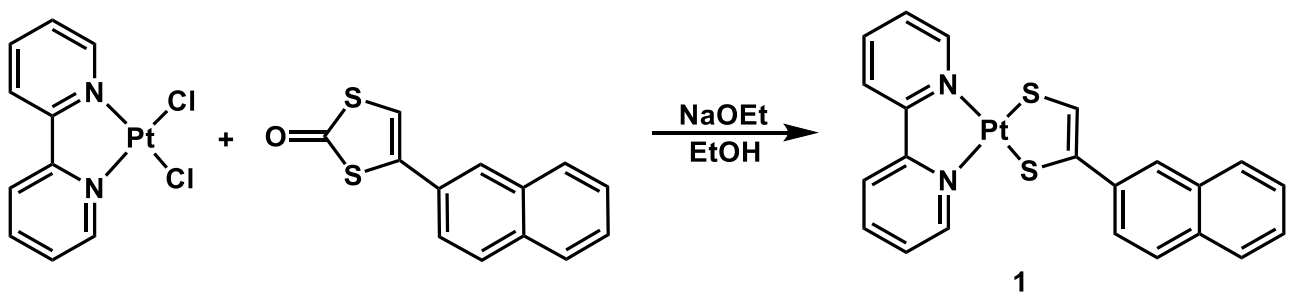
Atom number	Z	x	y	z	Atom number	Z	x	y	z
1	6	3.379106	2.709041	3.477204	87	6	0	-2.287964	0.169737
2	6	2.971888	2.199947	4.714354	88	6	0	-3.210285	1.068136
3	6	3.587588	1.068624	5.225584	89	6	0	-3.751827	0.820555
4	6	4.602248	0.459604	4.483517	90	6	0	-3.350953	-0.318576
5	6	4.952030	1.000865	3.258731	91	6	0	-2.428120	-1.169593
6	7	4.355395	2.097146	2.762023	92	7	0	-1.910081	-0.935722
7	1	2.165346	2.685659	5.261303	93	1	0	-3.496851	1.957110
8	1	3.280666	0.663471	6.192034	94	1	0	-4.480568	1.510261
9	1	5.119122	-0.431094	4.843650	95	1	0	-3.747393	-0.554790
10	1	5.733592	0.558455	2.636411	96	1	0	-2.083092	-2.073768
11	6	2.822367	3.916610	2.866298	97	6	0	-1.655261	0.341821
12	6	1.789687	4.669660	3.430486	98	6	0	-1.943673	1.395965
13	6	1.328709	5.798592	2.773448	99	6	0	-1.313081	1.455361
14	6	1.920108	6.156106	1.561730	100	6	0	-0.396068	0.458207
15	6	2.941837	5.371419	1.053631	101	6	0	-0.144819	-0.554381
16	7	3.387028	4.276767	1.687179	102	7	0	-0.756393	-0.611965
17	1	1.325560	4.345711	4.360400	103	1	0	-2.674215	2.151909
18	1	0.504799	6.381415	3.188808	104	1	0	-1.543101	2.266580
19	1	1.588341	7.032575	1.003158	105	1	0	0.124129	0.460254
20	1	3.425894	5.606791	0.102882	106	1	0	0.564367	-1.356811
21	78	4.775762	2.954495	0.948441	107	78	0	-0.507413	-2.103815
22	16	5.136861	4.032552	-1.014818	108	16	0	1.131512	-3.231016
23	16	6.147332	1.298329	0.216792	109	16	0	-0.463639	-3.736260
24	6	6.192561	2.978637	-1.891993	110	6	0	1.401905	-4.642721
25	6	6.638837	1.794514	-1.400696	111	6	0	0.730109	-4.899180
26	1	6.521564	3.351318	-2.866086	112	1	0	2.184896	-5.315304
27	6	7.519725	0.880389	-2.148776	113	6	0	0.927808	-6.118041
28	6	7.514618	0.834679	-3.535758	114	6	0	1.390327	-7.301152
29	6	8.370756	-0.026483	-4.263255	115	6	0	1.602603	-8.468943
30	6	9.258417	-0.892290	-3.551478	116	6	0	1.313896	-8.444806
31	6	9.245069	-0.845835	-2.133387	117	6	0	0.821872	-7.236994
32	6	8.409003	0.006414	-1.456458	118	6	0	0.634441	-6.117971
33	1	6.824682	1.470498	-4.097103	119	1	0	1.588377	-7.350930
34	6	8.371417	-0.069416	-5.683654	120	6	0	2.085788	-9.676174
35	6	10.110000	-1.759099	-4.282034	121	6	0	1.522216	-9.617509
36	1	9.924344	-1.499632	-1.579084	122	1	0	0.595924	-7.206534
37	1	8.425221	0.039688	-0.364673	123	1	0	0.259511	-5.195783
38	6	9.209507	-0.921319	-6.364648	124	6	0	2.278445	-10.797853
39	6	10.088691	-1.775292	-5.658057	125	6	0	1.995018	-10.770098
40	1	7.693492	0.592406	-6.230004	126	1	0	2.307089	-9.698028
41	1	9.199826	-0.939930	-7.457366	127	1	0	2.653728	-11.717285
42	1	10.751022	-2.447242	-6.209325	128	1	0	2.153047	-11.667265
43	1	10.788085	-2.417099	-3.731335	129	1	0	1.301106	-9.590625
44	6	2.588689	0.310488	-0.449194	130	6	0	-3.078058	-4.955346
45	6	3.449407	0.066555	-1.520323	131	6	0	-2.083327	-5.821379
46	6	3.490035	0.956829	-2.583150	132	6	0	-1.505536	-5.597438
47	6	2.670302	2.082976	-2.543347	133	6	0	-1.939739	-4.509309
48	6	1.827088	2.263475	-1.458592	134	6	0	-2.930056	-3.688324
49	7	1.774338	1.392722	-0.441772	135	7	0	-3.489360	-3.901938
50	1	4.099250	-0.806273	-1.510665	136	1	0	-1.748554	-6.652510
51	1	4.171674	0.782764	-3.417137	137	1	0	-0.714222	-6.253459
52	1	2.684636	2.829404	-3.338038	138	1	0	-1.509236	-4.287156
53	1	1.169981	3.132454	-1.384115	139	1	0	-3.296452	-2.819680
54	6	2.498777	-0.545520	0.734424	140	6	0	-3.754857	-5.102739
55	6	3.192214	-1.749316	0.876752	141	6	0	-3.468755	-6.113681
56	6	3.006700	-2.516544	2.015956	142	6	0	-4.179308	-6.178952
57	6	2.124608	-2.059843	2.993986	143	6	0	-5.167897	-5.222570

58	6	1.479423	-0.848592	2.804412	144	6	0	-5.395701	-4.236800
59	7	1.669311	-0.099991	1.709107	145	7	0	-4.707447	-4.172657
60	1	3.845621	-2.094974	0.078155	146	1	0	-2.678043	-6.833284
61	1	3.520291	-3.473151	2.126832	147	1	0	-3.961485	-6.961765
62	1	1.924850	-2.639707	3.896073	148	1	0	-5.757720	-5.233339
63	1	0.771820	-0.457490	3.538943	149	1	0	-6.146541	-3.457616
64	78	0.649449	1.626969	1.259964	150	78	0	-4.877976	-2.682187
65	16	-0.423275	1.830772	3.262179	151	16	0	-6.378093	-1.422095
66	16	-0.543173	3.414915	0.510650	152	16	0	-4.804223	-1.042453
67	6	-1.503718	3.168890	3.025128	153	6	0	-6.502177	0.039650
68	6	-1.588868	3.859052	1.859945	154	6	0	-5.828777	0.242458
69	1	-2.107687	3.445416	3.894314	155	1	0	-7.193073	0.789921
70	6	-2.545960	4.956434	1.630402	156	6	0	-5.869644	1.502260
71	6	-3.767325	5.005496	2.286986	157	6	0	-6.005419	2.729225
72	6	-4.694488	6.053722	2.073032	158	6	0	-6.041585	3.948360
73	6	-4.373374	7.091668	1.143302	159	6	0	-5.924006	3.919256
74	6	-3.126387	7.024747	0.469682	160	6	0	-5.773592	2.658264
75	6	-2.247021	5.996496	0.700948	161	6	0	-5.743621	1.493561
76	1	-4.043995	4.203333	2.976048	162	1	0	-6.070867	2.771481
77	6	-5.949650	6.100002	2.738202	163	6	0	-6.173708	5.205489
78	6	-5.310048	8.132918	0.920574	164	6	0	-5.956280	5.140493
79	1	-2.873367	7.809946	-0.248150	165	1	0	-5.689556	2.625194
80	1	-1.292882	5.959584	0.169837	166	1	0	-5.636759	0.531271
81	6	-6.839322	7.121355	2.498589	167	6	0	-6.200227	6.373349
82	6	-6.517466	8.149751	1.581570	168	6	0	-6.093044	6.342420
83	1	-6.198676	5.305860	3.447622	169	1	0	-6.251221	5.234625
84	1	-7.800748	7.141841	3.017704	170	1	0	-6.305098	7.330214
85	1	-7.231595	8.956650	1.400225	171	1	0	-6.118747	7.276763
86	1	-5.055819	8.925311	0.210901	172	1	0	-5.871851	5.111167

Table S4. Energy E (eV), wavelength λ (nm), and oscillator strength f of main ($f \geq 0.005$) electronic transitions calculated in the Vis–NIR (500–850 nm) for **2** in the gas phase, along with molecular orbital composition of the excited-state functions and complex monomers where the involved KS-MOs are mainly localized.

ES	E	λ	f	Composition	%	Monomers ^a
1	1.507	823.0	0.023	H→L+1	80	d(84%)→ d(93%)
2	1.524	813.5	0.023	H-1→L	67	a(70%)→a(98%)
3	1.702	728.6	0.021	H-3→L	12	b(52%)→ a(98%)
				H-2→L	27	c(52%)→ a(98%)
				H-1→L+2	24	a(70%)→b(89%)
				H→L	21	d(84%)→ a(98%)
				H-1→L	13	a(70%)→ a(98%)
				H-3→L	12	b(52%)→ a(98%)
4	1.719	721.2	0.045	H-2→L+1	40	c(52%)→ d(93%)
				H→L+3	23	d(84%)→c(84%)
				H→L+2	16	d(84%)→ b(89%)
				H-3→L+1	10	b(52%)→ d(93%)
5	1.746	709.9	0.013	H→L	42	d(84%)→ a(98%)
				H-1→L+2	18	a(70%)→ b(89%)
				H→L+2	12	d(84%)→ b(89%)
6	1.769	701.0	0.023	H→L	24	d(84%)→ a(98%)
				H→L+2	15	d(84%)→ b(89%)
				H-2→L+2	13	c(52%)→ b(89%)
				H-2→L+1	12	c(52%)→ d(93%)
				H-3→L	10	b(52%)→ a(98%)
				H-2→L	9	c(52%)→ a(98%)
7	1.809	685.6	0.130	H-1→L+2	45	a(70%)→ b(89%)
				H-2→L	12	c(52%)→ a(98%)
				H-1→L	10	a(70%)→ a(98%)
8	1.832	676.9	0.064	H→L+3	49	d(84%)→ c(84%)
				H-2→L+2	27	c(52%)→ b(89%)
9	1.870	663.1	0.012	H-1→L+1	44	a(70%)→ d(93%)
				H-3→L+1	16	b(52%)→ d(93%)
				H-1→L+3	14	a(70%)→ c(84%)
11	1.950	636.0	0.006	H-1→L+1	27	a(70%)→ d(93%)
				H-2→L+2	18	c(52%)→ b(89%)
				H→L+2	17	d(84%)→ b(89%)
				H-1→L+3	11	a(70%)→ c(84%)
12	1.994	621.9	0.006	H→L+2	26	d(84%)→ b(89%)
				H-2→L+2	20	c(52%)→ b(89%)
				H-3→L+2	14	b(52%)→ b(89%)
				H-1→L+3	13	a(70%)→ c(84%)
13	2.037	608.7	0.044	H-3→L+2	38	b(52%)→ b(89%)
				H-3→L+1	32	b(52%)→ d(93%)
				H-2→L+1	13	c(52%)→ d(93%)
14	2.067	599.8	0.045	H-3→L+2	31	b(52%)→ b(89%)
				H-3→L+1	27	b(52%)→ d(93%)
				H-1→L+3	21	a(70%)→ c(84%)
15	2.115	586.3	0.060	H-2→L+3	56	c(52%)→ c(84%)
				H-3→L+3	30	b(52%)→ c(84%)
				H-1→L+3	10	a(70%)→ c(84%)
17	2.373	522.5	0.007	H→L+5	95	d(84%)→d(96%)
18	2.401	516.4	0.006	H-1→L+4	93	a(70%)→ a(96%)

^a Labelling of monomers as in Figure S5.



Scheme S1. Synthetic pathway for the preparation of complex **1** from [Pt(bipy)Cl₂] and 4-(2-naphthyl)-[1,3]dithiol-2-one.

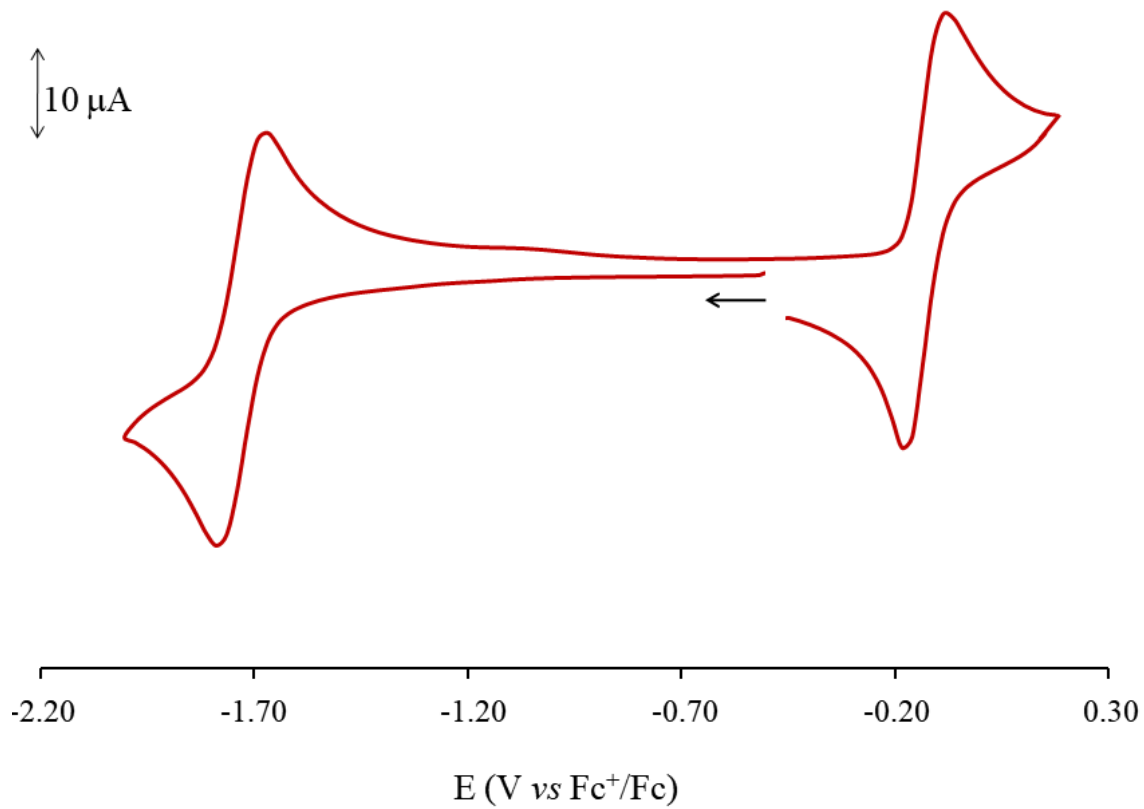


Figure S1. Cyclic voltammogram of **1** recorded in anhydrous DMSO at 298 K (scan rate 100 mV s⁻¹; 0.1 M TBAPF₆).

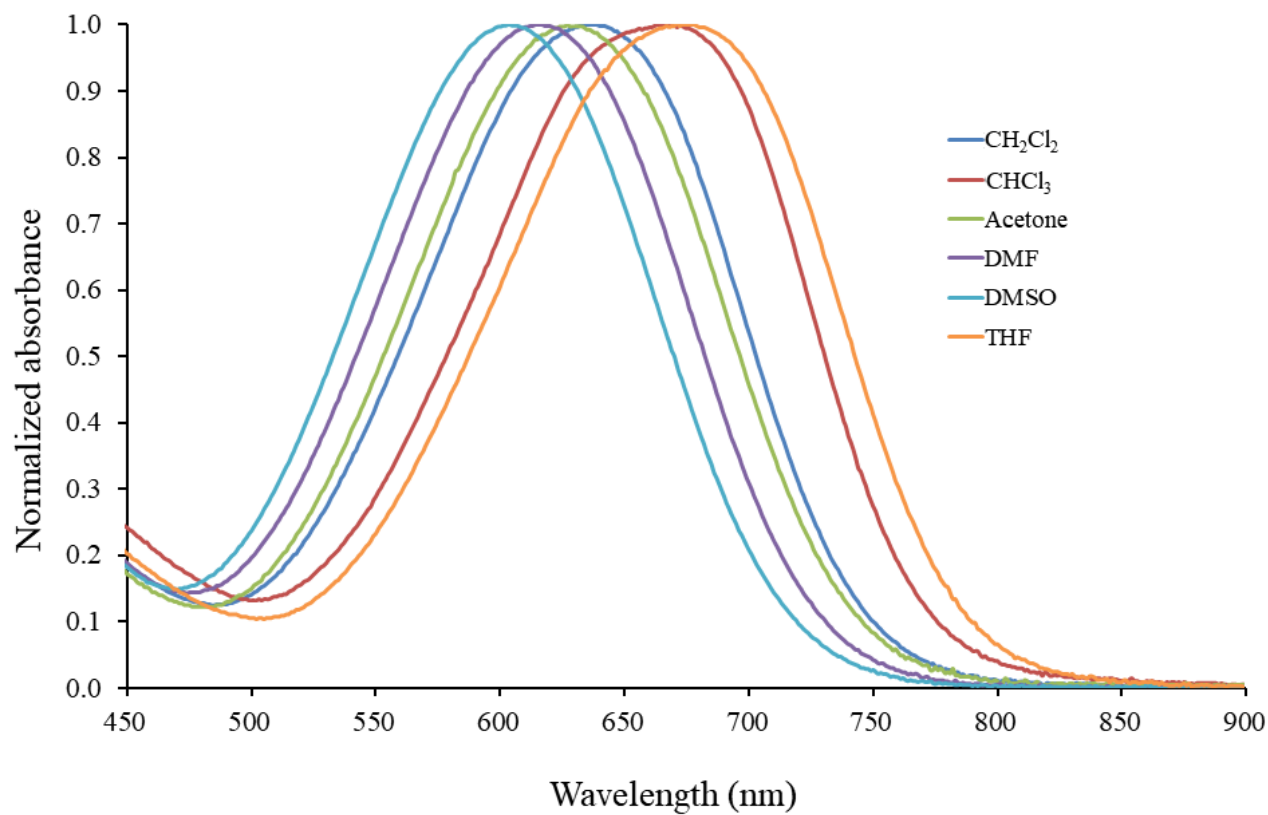


Figure S2. Normalized absorption spectra in the Vis region (450–900 nm) recorded for **1** in selected solvents at 298 K. λ_{\max} values: MeCN, 600 nm; DMSO, 603 nm; DMF, 617 nm; acetone, 625 nm; CH_2Cl_2 , 642 nm; CHCl_3 , 666 nm; THF, 672 nm; toluene, 700 nm. The spectra in MeCN and toluene, of very low quality because of solubility reasons, are not depicted.

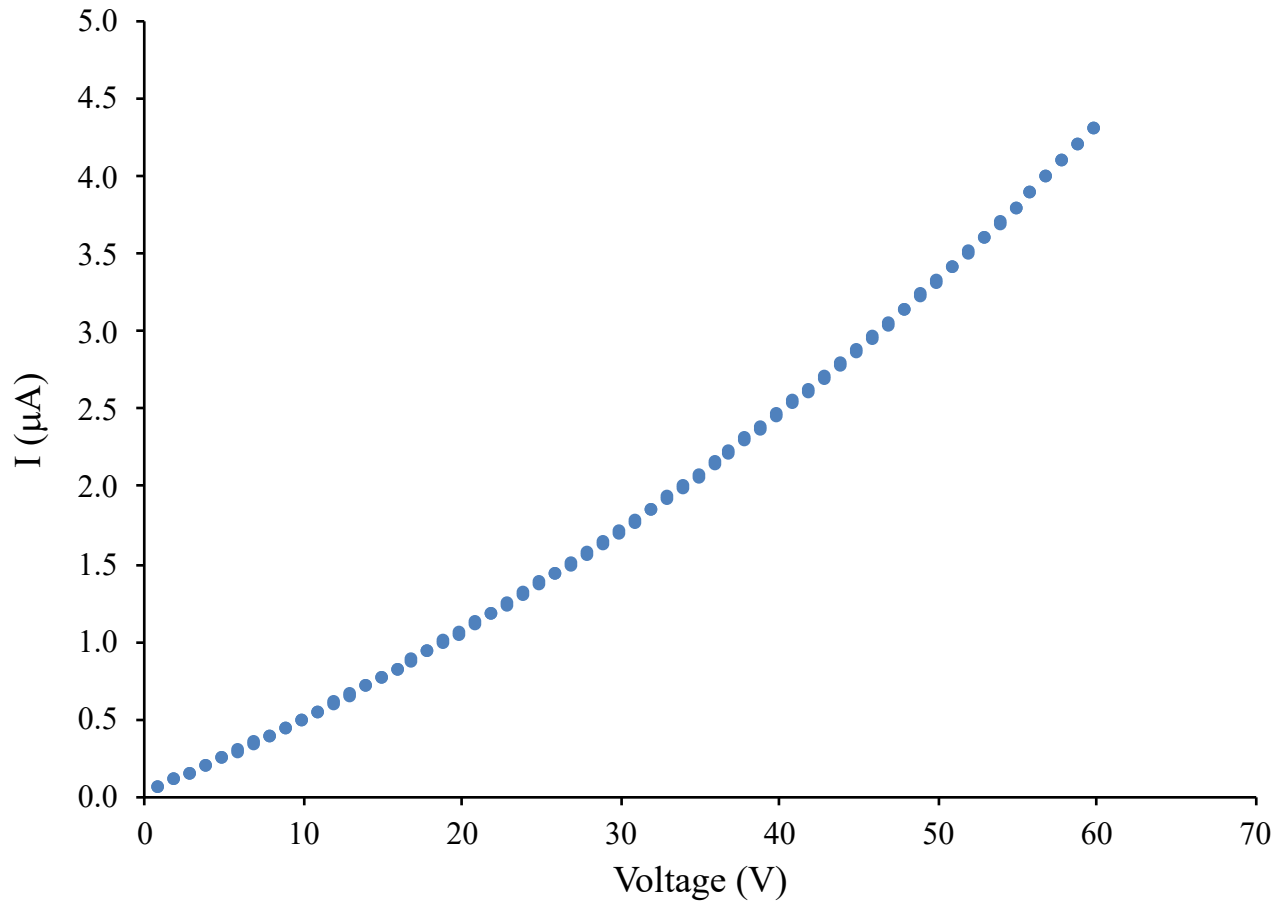


Figure S3. Dark current of the prototype photodetector.

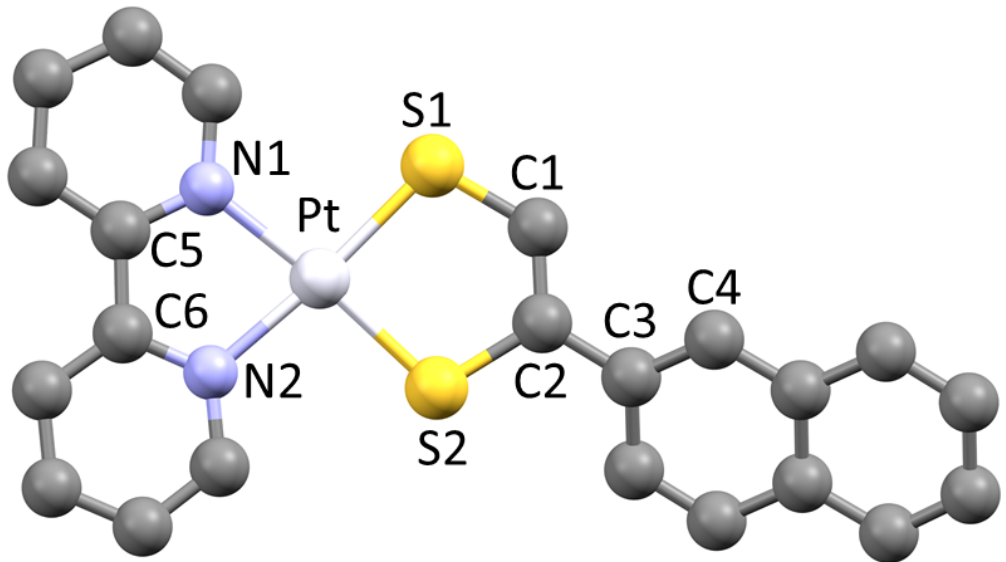


Figure S4. Molecular drawing and atom labelling scheme of **1** at the optimized geometry in the gas phase; hydrogen atoms omitted for clarity.

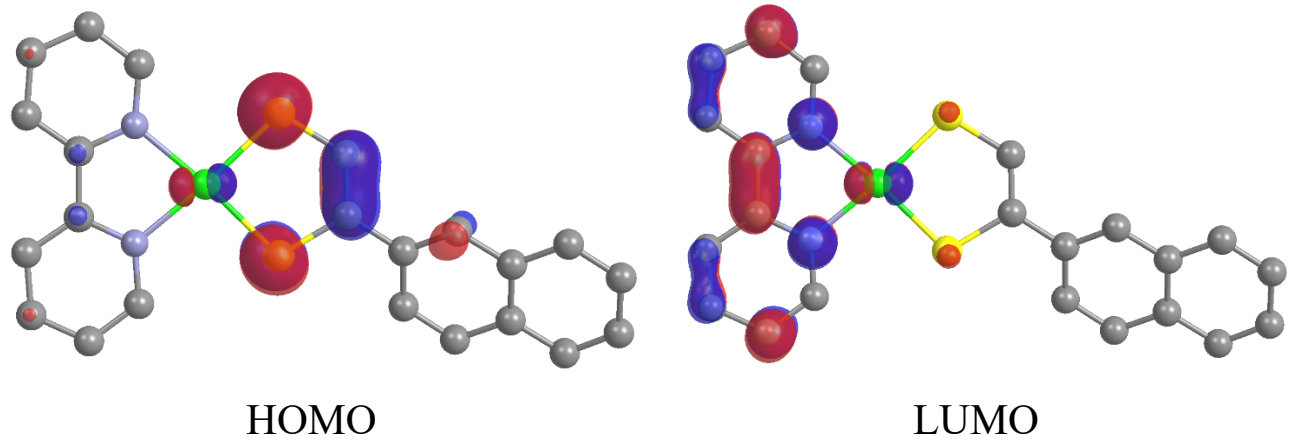


Figure S5. Isosurface drawings of the frontier Kohn–Sham molecular orbitals calculated for **1** at the optimized geometry. Hydrogen atoms were omitted for clarity. Cutoff value = 0.05 |e|.

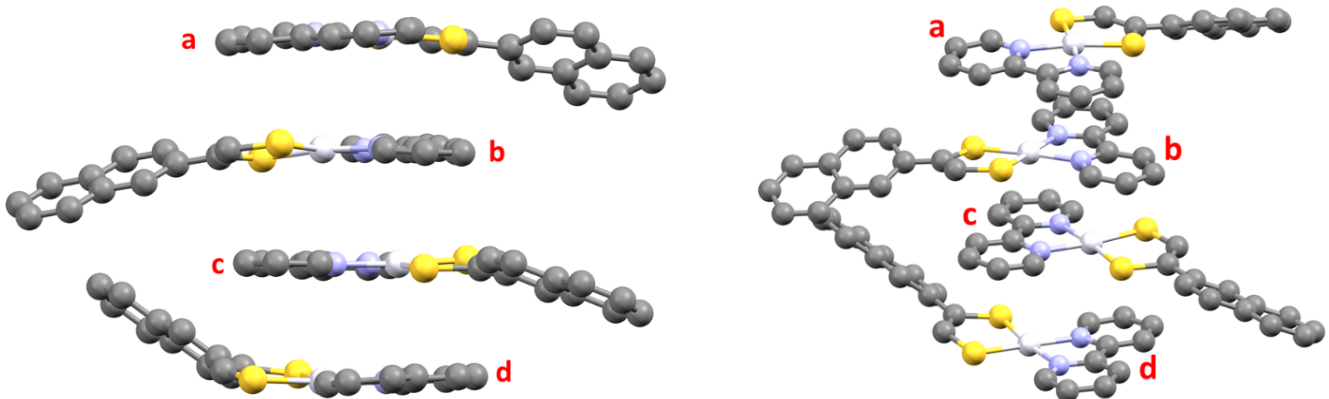


Figure S6. Different views of **2** at the optimized geometry in the gas phase, with complex units labelling scheme; hydrogen atoms omitted for clarity.

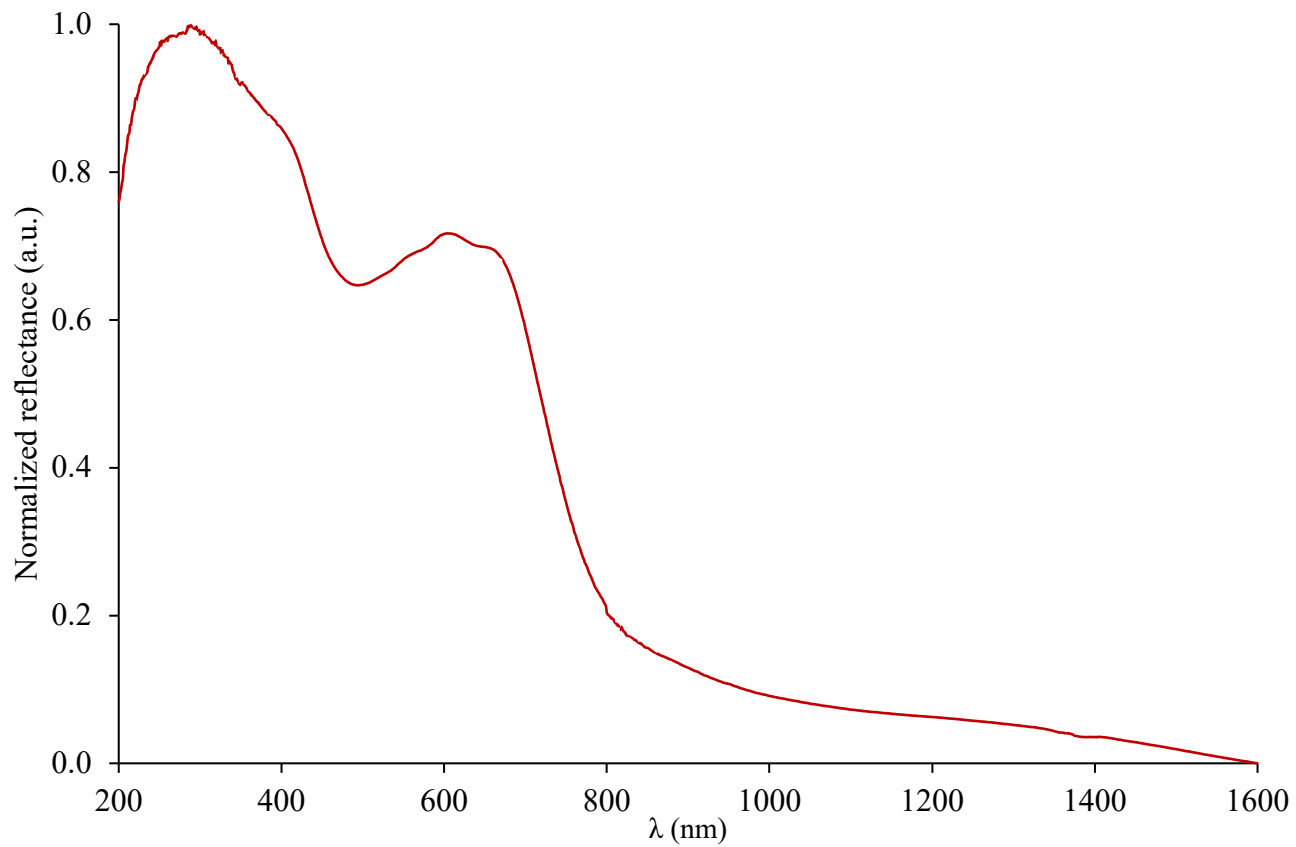


Figure S7. Solid state diffuse reflectance spectrum recorded for **1** in the range 200–1600 nm.

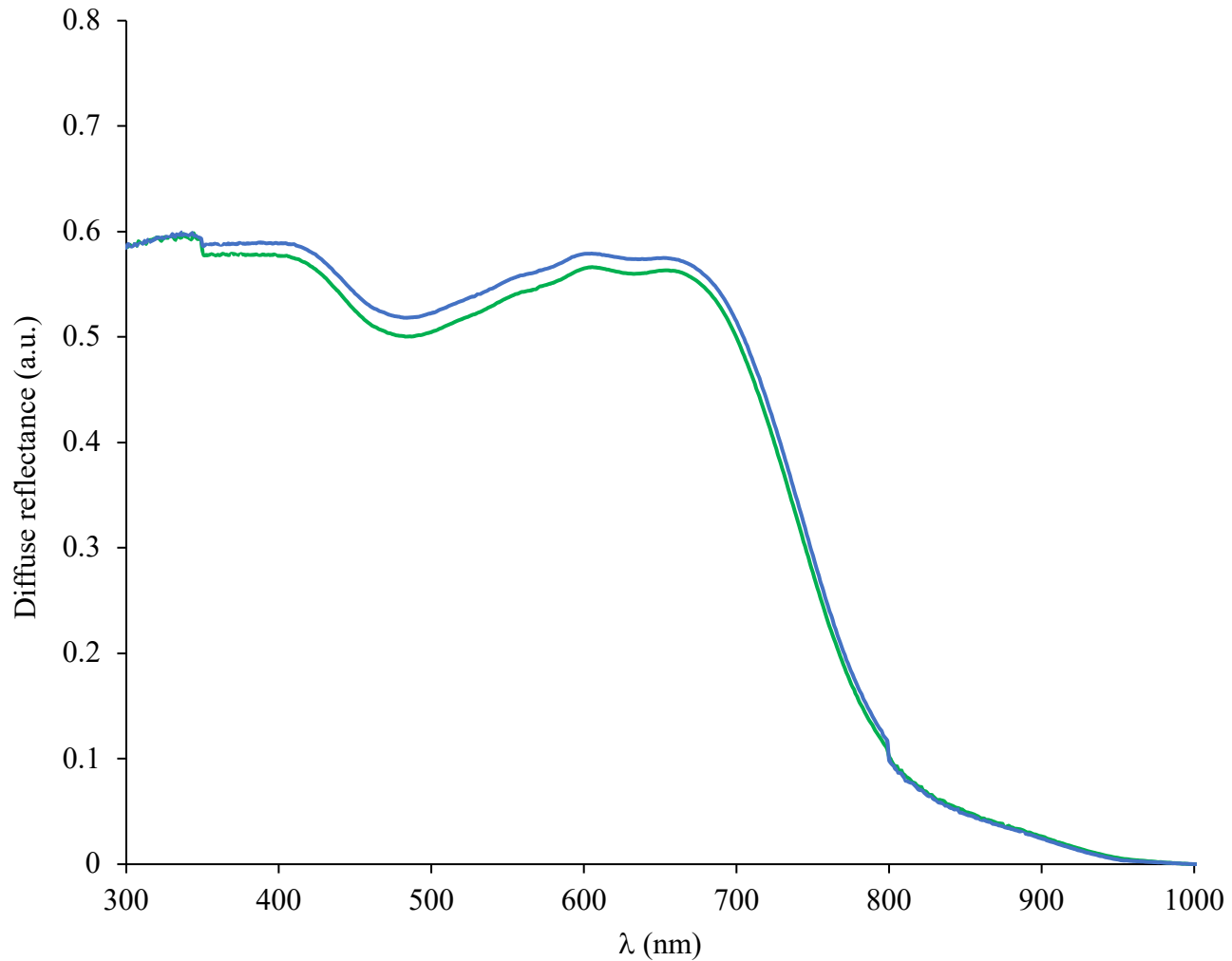


Figure S8. Baseline corrected unscaled solid state diffuse reflectance spectra recorded for **1** in the range 300–1000 nm before (green) and after (blue) continuous laser irradiation ($\lambda = 650$ nm; 30 mW/cm^2). Small intensity variations are attributed to the repositioning of the sample in the integration sphere.

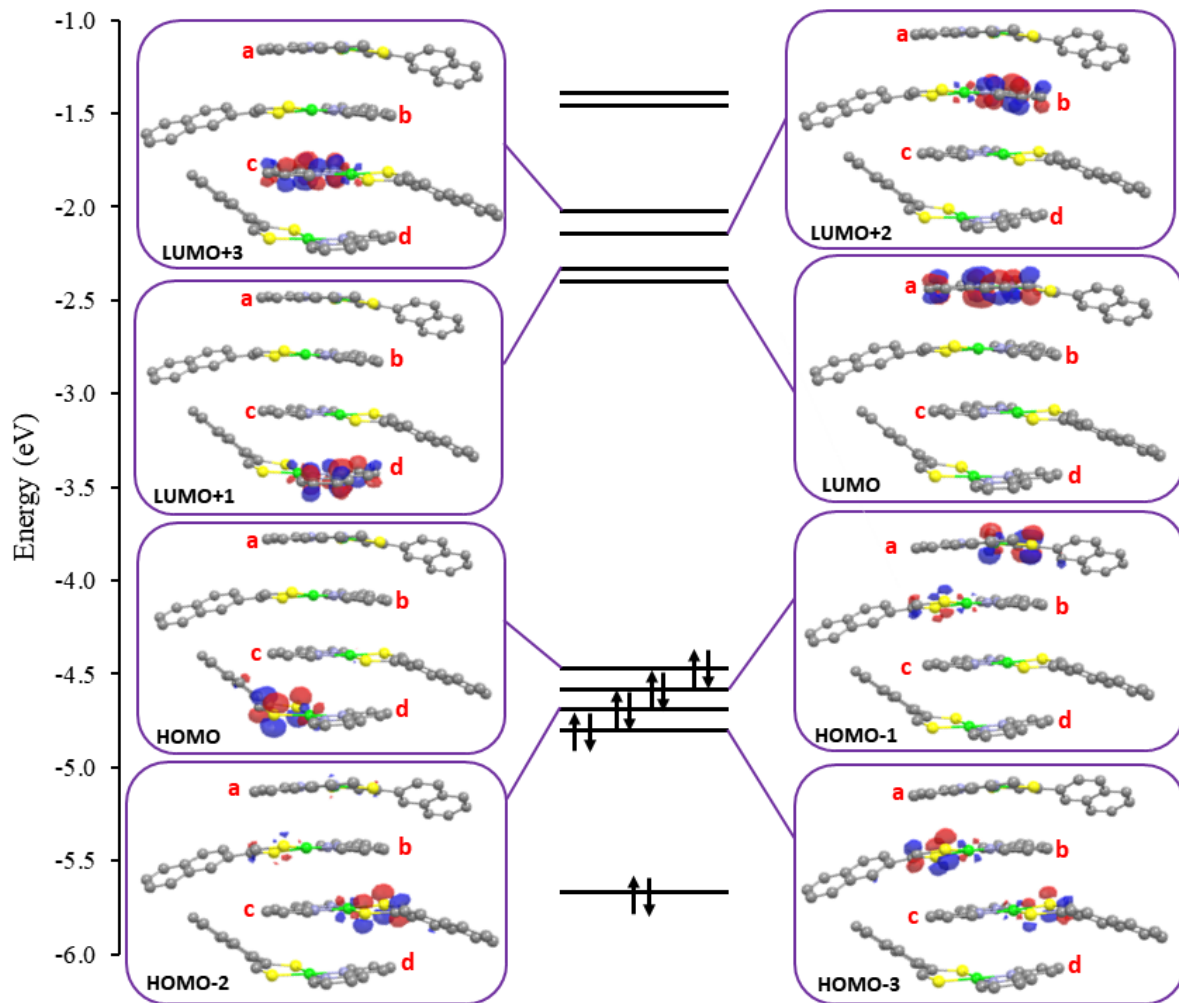


Figure S9. KS-MOs diagram with isosurface drawings calculated for **2** in the gas phase (contour value 0.05 |e|; hydrogen atoms omitted for clarity).

REFERENCES

- 1 A. Pintus, M. C. Aragoni, N. Bellec, F. A. Devillanova, D. Lorcy, F. Isaia, V. Lippolis, R. A. M. Randall, T. Roisnel, A. M. Z. Slawin, J. D. Woollins and M. Arca, *Eur. J. Inorg. Chem.*, 2012, **2012**, 3577–3594.
- 2 L. Ambrosio, M. C. Aragoni, M. Arca, F. A. Devillanova, M. B. Hursthouse, S. L. Huth, F. Isaia, V. Lippolis, A. Mancini and A. Pintus, *Chem. Asian J.*, 2010, **5**, 1395–1406.
- 3 G. T. Morgan and F. H. Burstall, *J. Chem. Soc.*, 1934, 965–971.
- 4 W. B. Connick and H. B. Gray, *J. Am. Chem. Soc.*, 1997, **119**, 11620–11627.
- 5 W. Koch and M. C. Holthausen, *A chemist's guide to density functional theory*, Wiley-VCH, New York, 2001.
- 6 Gaussian 16 Rev. B. 01, M. J. Frisch, G. W. Trucks, H. B. Schlegel, G. E. Scuseria, M. A. Robb, J. R. Cheeseman, G. Scalmani, V. Barone, G. A. Petersson, H. Nakatsuji, X. Li, M. Caricato, A. V. Marenich, J. Bloino, B. G. Janesko, R. Gomperts, B. Mennucci, H. P. Hratchian, J. V. Ortiz, A. F. Izmaylov, J. L. Sonnenberg, D. Williams-Young, F. Ding, F. Lipparini, F. Egidi, J. Goings, B. Peng, A. Petrone, T. Henderson, D. Ranasinghe, V. G. Zakrzewski, J. Gao, N. Rega, G. Zheng, W. Liang, M. Hada, M. Ehara, K. Toyota, R. Fukuda, J. Hasegawa, M. Ishida, T. Nakajima, Y. Honda, O. Kitao, H. Nakai, T. Vreven, K. Throssell, J. A. Montgomery, J. E. Peralta, F. Ogliaro, M. J. Bearpark, J. J. Heyd, E. N. Brothers, K. N. Kudin, V. N. Staroverov, T. A. Keith, R. Kobayashi, J. Normand, K. Raghavachari, A. P. Rendell, J. C. Burant, S. S. Iyengar, J. Tomasi, M. Cossi, J. M. Millam, M. Klene, C. Adamo, R. Cammi, J. W. Ochterski, R. L. Martin, K. Morokuma, O. Farkas, J. B. Foresman and D. J. Fox, Wallingford, CT, 2016.
- 7 C. Adamo and V. Barone, *J. Chem. Phys.*, 1999, **110**, 6158–6170.
- 8 A. Schäfer, H. Horn and R. Ahlrichs, *J. Chem. Phys.*, 1992, **97**, 2571–2577.
- 9 F. Weigend and R. Ahlrichs, *Phys. Chem. Chem. Phys.*, 2005, **7**, 3297–3305.
- 10 W. C. Ermler, R. B. Ross and P. A. Christiansen, *Int. J. Quantum Chem.*, 1991, **40**, 829–846.
- 11 T. H. Dunning and P. J. Hay, in *Modern theoretical chemistry*, Plenum Press, New York, 1977, vol. 3, p. 1.

- 12 K. L. Schuchardt, B. T. Didier, T. Elsethagen, L. Sun, V. Gurumoorthi, J. Chase, J. Li and T. L. Windus, *J. Chem. Inf. Model.*, 2007, **47**, 1045–1052.
- 13 A. E. Reed, R. B. Weinstock and F. Weinhold, *J. Chem. Phys.*, 1985, **83**, 735–746.
- 14 *GaussView 6.0.16*, R. D. Dennington, T. A. Keith and J. M. Millam, *Semichem*, Inc., Shawnee Mission KS, 2016.
- 15 G. Schaftenaar and J. H. Noordik, *J. Comput. Aided. Mol. Des.*, 2000, **14**, 123–134.
- 16 L. V Skripnikov, *Chemissian Version 4.53, Visualization Computer Program*, 2017.
- 17 N. M. O’Boyle, A. L. Tenderholt and K. M. Langner, *J. Comput. Chem.*, 2008, **29**, 839–845.